Natural Hazards
https://doi.org/10.1007/s11069-021-04523-0

ORIGINAL PAPER

Spatiotemporal variability of multifractal properties of fineresolution daily gridded rainfall fields over India

Adarsh Sankaran[1] · Sagar Rohidas Chavan[2] · Mumtaz Ali[3] · Archana Devarajan Sindhu[1] · Drisya Sasi Dharan[1] · Muhammad Ismail Khan[4]

Received: 27 October 2020 / Accepted: 8 January 2021

Abstract
This study investigated the multifractal characteristics of fine resolution (0.25°x0.25°) daily gridded rainfall fields of India over the period 1901–2013 to examine their spatiotemporal variability. The scaling characterization using Multifractal Detrended Fluctuation Analysis (MFDFA) detected short-term persistency and strong multifractality in the majority of rainfall (over 81%) of the grid points. A detailed exploration on the spatial variability of multifractal properties such as Hurst exponent, spectral width, asymmetry index, Hölder exponent are also performed for six rainfall homogenous regions and 34 meteorological subdivisions in India. The results showed that the highest persistence and complexity is noted in the mountainous terrains of northern and northeastern India. The sub-divisional scale analysis showed that the variability of persistence and complexity is the highest in Kerala and lowest at Vidarbha. Further, the evaluation of multifractal properties of rainfall series of pre- and post-1976/77 Pacific climate shift showed an increase in strength of multifractality in 62% grids after the shift. Changes in the status of persistence with respect to 1976/77 is the highest at Uttaranchal subdivision and changes from positive to negative asymmetry was the highest at northwestern (NW) region. Grid points of Peninsular India exhibited least reduction in complexity, multifractality and persistence in the post-1977 period when compared to pre-1977 period.

Keywords Multifractal · Rainfall · Correlation · Climate shift · Persistence · Complexity

1 Introduction

Climate change and the inherent perturbations in any climate variable can significantly affect rainfall patterns, which may impact agriculture, water resources, escalates unusual calamities due to hydrological extremes like floods or droughts and eventually affect economic growth (Bhalme and Mooley 1980; Langridge et al. 2006; Barredo, 2007; Vörösmarty et al. 2010; Ali et al. 2018a, 2018b, 2019). Considering these, the accurate prediction, development of climate risk evaluations and relevant mitigation and adaption

✉ Mumtaz Ali
mumtaz.ali@deakin.edu.au

Extended author information available on the last page of the article

measures require in-depth understanding of the characteristics of the time series. The estimation of fluctuations and persistence of hydrological time series are vital steps in the time series characterization, but it is a challenging problem in time series analysis. Harold Edwin Hurst is one of the first contributors in this field and the classical Rescaled Range (R/S) analysis might be the first quantitative information on persistence of time series (Hurst 1951). The conceptual development of 'fractal' theory in 1970s helped for the better understanding on the characteristic analysis of complex time series in different scientific disciplines. The fractality can be referred as the property of a fragmental geometrical object that can be subdivided into parts, each of which is a reduced size copy of the whole (Mandelbrot 1982). Fractal properties are considered as the identity or signatures of the time series and researchers have widely applied this concept in biomedical, financial, geophysical, and environmental time series in the past few decades (Kandelhardt et al. 2006; Ihlen 2012).

Many of the complex hydrological time series often exhibit self-similarity or self-affinity and scale invariance over certain range of time scales which are typical characteristics of fractals (Shang and Kame 2005). Under the turbulent environment, such time-series signals can be considered as analogous to stochastic cascade models. To demonstrate such phenomenon of flux transfer, the classical scaling laws were proposed (Kolmogorov 1941; Obukhov 1949). This laid a foundation for the determination of fractal behavior of time series, but such flux transfer need not be homogenous, instead intermittent in many of the hydrological variables like rainfall (Verrier et al. 2010). To address such issues, the alternate scaling cascade models were proposed (Mandelbrot 1982) and such models were adapted to reproduce scale invariance properties using fractal geometry. For the detection of fractality of time series signals, numerous methods were proposed in the past. The classical box counting algorithm (Mandelbrot 1982), Fourier spectral analysis (used by Pandey et al. 1998), extended self-similarity (ESS) method (Dahlstedt and Jensen 2005) and classical structure function analysis (Schertzer and Lovejoy 1987) were some of them. The estimate of scaling exponents based on such algorithms may be influenced more by the periodic components and trends (Kantelhardt et al. 2006; Huang et al. 2009) which are evidently present in hydrological time series. To address such issues, an algorithm with detrending operation is more appropriate and the Detrended Fluctuation Analysis (DFA) propounded by Peng et al. (1994) was one of the earlier attempts in this direction. Later on, it was recognized that it is necessary to use multiple scaling exponents to describe the complex geophysical processes and accordingly, many multifractal formalisms were proposed (Tessier et al. 1993, 1996; Pandey et al. 1998; Kantelhardt et al. 2003). The Multifractal Detrended Fluctuation Analysis (MFDFA) presented by Kantelhardt et al. (2002) was recognized as a major breakthrough in this field. Because of its ability to distinguish between long-term correlations and trends and simplicity in implementation, the MFDFA method gained wide popularity in hydrological applications (Kantelhardt et al. 2006; Koscielny-Bunde et al. 2006; Zhang et al. 2008, 2009; Rego et al. 2013; Li et al. 2015; Tan and Gan 2017; Hou et al. 2018; Adarsh et al. 2018, 2020). Multifractal properties can be considered as '*fingerprint*' of the hydrological series and it serves as an efficient non-trivial test bed for evaluating the performance of rainfall-runoff models (Kantelhardt et al. 2006). The detection of multifractal properties of rainfall time series may be helpful to proceed with many practical hydrological applications like multifractal modeling of rainfall, generation of synthetic rainfall, de-noising of hydrological signals, homogeneity detection (Deidda et al. 1999, 2000; Deidda 1999, 2000; Serinaldi 2010; Garcia-Marin et al. 2015, 2019). Multifractal models with different frameworks could be developed for simulating or predicting different hydrological variables including rainfall (Tessier et al. 1996; Kandelhart

et al. 2003, 2006). The exponents can also be used for developing Intensity–Duration–Frequency curves of rainfall, which are one of most widely used practical hydrological tool for storm water drainage systems (Veneziano and Furcolo 2002; Huang et al. 2014). The spatiotemporal disaggregation of rainfall is another promising application of the derived exponents (Hubert 2001; Pathirana et al. 2007). For such a wide range of practical usefulness and extension studies, the determination of fractal (or multifractal) properties is an essential prerequisite.

The fractality description and self-similarity or scaling concepts were applied for stochastic generation and disaggregation of rainfall (Olsson and Niemczynowicz 1996; Tessier et al. 1996). Kantelhardt et al. (2003) investigated the multifractality of streamflow and rainfall data of diverse temporal scales collected from different parts of the world. The results obtained by MFDFA method were compared with that by wavelet transform modula maxima method. The results by both methods displayed good concurrence and they reported a non-universal behavior of scaling exponents and multifractality in the rainfall time series. The classical contribution by Kantelhardt et al. (2006), investigated the multifractality of 99 rainfall time series and 42 runoff series at daily time scale, compiled from diverse locations of the globe. They reported short term persistence (STP) in rainfall data and long-term persistence (LTP) in runoff data with a mean scaling exponent of ~ 0.53 and ~ 0.73 respectively. Yu et al. (2014) determined the multifractal characteristics of daily rainfall series from different meteorological stations in Pearl River basin, China. They followed MFDFA and universal multifractal approach for the characterization. They confirmed multifractality by both the methods, but in two distinctly different time scale ranges and the former method reported short-term correlations in the datasets. Their study also investigated the association of rainfall variability with topography and negative correlations in the rainfall-elevation relationships.

Additionally, Baranowski et al. (2015) determined the scaling behavior of daily air temperature, wind velocity, relative air humidity, global radiation, and rainfall time series of 31-year length, collected from meteorological stations of Finland, Germany, Poland and Spain. In majority of the time series, long-range correlations were the reason for multifractality, but for the rainfall series multifractality was resulted from broadness of probability distribution. Tan and Gan (2017) applied MFDFA for description of multifractality of daily scale streamflow time series (145 numbers) and rainfall time series (100 numbers) of Canada. They confirmed that all the rainfall series showed LTP irrespective of the range of time scales, but streamflow displayed LTP mainly at large time scales. Krzyszczak et al. (2018) used MFDFA to investigate the multifractality of different meteorological time series recorded at four stations in Bulgaria and Poland, with diverse climatic characteristics. Daily time series comprising over 11,000 data points of rainfall (mm), wind speed (ms^{-1}), air temperature (°C) and relative humidity (%) were considered in the study. It was reported that the multifractal property of rainfall differs significantly from that of other variables. Each series was split into two with respect to the climatic shift of 2001/2002 and multifractality was analyzed. The singularity spectra were found to be susceptible to climatic shift and the change was apparent for asymmetry. There was a right- to left-skewed switchover in the asymmetry of the spectra, which implies the presence of frequent extreme events in the regions in recent past.

Some very recent studies investigated the multifractality of rainfall and rainfall derived drought index (Standardized Precipitation Index, SPI) series in the Indian context (Adarsh et al. 2019, 2020). However, they used coarse resolution data to get a broader overview on multifractality of rainfall fields in India. These studies highlighted the importance of multifractal analysis of rainfall in India using more fine resolution

data and investigating the spatiotemporal variability of these properties to get a better insight in the context of climatic changes. Motivated from the literature, the specific objectives of the study are designed as follows:

1. To perform multifractal analysis for fine resolution (0.25°x 0.25°) daily gridded rainfall time series from India
2. To examine the spatiotemporal changes in the multifractal properties of daily gridded rainfall data of India.

In the next section, the theoretical background of MFDFA is presented. In Sect. 3, the study area and data details are presented. Section 4 presents the results of application of MFDFA on the finer scale rainfall data and in-depth analysis of spatiotemporal variability of extracted multifractal parameters along with relevant discussions. The final section presents the concluding remark.

2 Theoretical background of methodology

2.1 Multifractal detrended fluctuation analysis

The multifractal detrended fluctuation analysis (MFDFA) is one of the well-accepted mathematical procedure for detection of the scaling behaviors and multifractality of nonlinear and non-stationary time series. The different steps of MFDFA algorithm are (modified from Kantelhardt et al. 2006; Zhang et al. 2009; Li et al. 2015):

1. In the first step, the 'profile' (accumulated deviation of the series from the mean) is of a time series X ($x_1, x_2 \ldots x_N$), N is the length of the time series is determined as (modified from Li et al. 2015):

$$P(i) = \sum_{k=1}^{i} \left[x_k - \left\langle \bar{x} \right\rangle \right] \tag{1}$$

   where $i = 1, 2, \ldots, N$, $\left\langle \bar{x} \right\rangle$ is the mean of the time series.
2. The profile $P(i)$ is divided into $N_s = \text{int}(N/s)$ non-overlapping segments length. Here, s is the segment sample size (popularly called as '*scale*') and 'int' refers the integer part. To avoid possible omission of datasets from the tail end of the series (as N need not be a multiple of s), the division process is performed also starting from the tail end, bringing $2N_s$ segments in total.
3. The local trends in each segment are calculated by least square fits of the series. Subsequently, the fluctuations in the series are computed as (modified from Kantelhardt et al. 2006):

$$FF^2(s,k) = \frac{1}{s} \sum_{i=1}^{s} \left\{ P[(k-1)s + i] - Y_k(i) \right\}^2 \text{ for } k = 1, 2, \ldots, N_s \tag{2}$$

   and

$$FF^2(s,k) = \frac{1}{s}\sum_{i=1}^{s}\left\{P[N-(k-N_s)s+i] - Y_k(i)\right\}^2 \text{ for } k = N_s+1, ..., 2N_s \tag{3}$$

Here, $Y_k(i)$ is the polynomial used for fitting the kth segment, which can be of any order like linear, quadratic, cubic.

4. The fluctuation function for different statistical moment order q (other than zero), can be determined as (modified from Kantelhardt et al. 2006):

$$FF_q(s) = \left\{\frac{1}{2N_s}\sum_{k=1}^{2N_s}\left[FF_q^2(s,\,k)\right]^{q/2}\right\}^{1/q} \tag{4}$$

For $q=0$, the fluctuation function is computed by the following expression (modified from Kantelhardt et al. 2002):

$$FF_0(s) = \exp\left\{\frac{1}{4N_s}\sum_{v=1}^{2Ns}\ln[FF^2(s,\,k)]\right\} \tag{5}$$

5. The logarithmic plots of $FF_q(s)$ versus scale for different values of q are prepared. If the series is power law correlated, the relation $FF_q(s) \sim s^{h(q)}$ exists and $h(q)$ is called as the Generalized Hurst Exponent (GHE).

GHE for $q=2$ (i.e., $h(2)$), which lies between 0 and 1 for stationary series, is considered to be equivalent to the classical Hurst exponent (H). A Hurst exponent (H) value between 0.5 and 1 designates LTP (long-memory process) and H between 0 and 0.5, designates STP (short-memory process). The series is deemed to be uncorrelated if H takes a value equal to 0.5 (Zhang et al. 2009). The long memory persistence characterizes positive autocorrelation in the time series (i.e., the effect of a typical data value on future values remains considerably for a longer time period). This is notable even in hydrological extremes in such a way that there is a likely chance that an extreme event will be followed by another extreme of similar character (i.e., a flood event followed by another similar event). The appropriate selection of moment orders, type of polynomial function, scale range (minimum s—maximum s) are some of the main issues in the implementation of MFDFA algorithm. Ihlen (2012) have given some quantitative guidelines for choosing the algorithm specific parameters for the implementation of MFDFA algorithm. To prevent plausible errors in the estimation of local fluctuations, the minimum scale can be chosen sufficiently larger than the order of the polynomial and maximum scale can be selected as a value less than half of the data length (Ihlen 2012). The order of the polynomial can be fixed between 1 and 3 to eliminate possible overfitting issues in segments of smaller length.

The q-order dependency of GHE indicates multifractality of the series and the scaling exponent computed for $q=2$ (i.e., $h(2)$) is helpful in commenting on persistence of the series (Kantelhardt et al. 2006). From the function of GHE, different useful exponents can be developed to comment on the multifractality and complexity of the time series. The mass exponent ($\tau(q)$) can be derived from GHE and subsequent differentiation of mass exponent may help in estimation of singularity exponent (α). These are two popular multifractal exponents, the methods of estimation of these exponents are available in the literature (Zhang et al. 2009). The function comprising the above two exponents indicated as $f(\alpha)$ can be plotted against α to get the singularity spectrum (multifractal spectrum). The base width of the multifractal spectrum depicts the degree of multifractality of the

time series. A wider spectrum depicts higher strength of multifractality of the time series and vice versa. The singularity spectrum will be parabola with maximum value of $f(\alpha)$ as unity. The left and right limbs of this inverted parabola correspond to negative and positive q respectively. Asymmetry Index (AI) is another prominent multifractal property derived from the shape of the multifractal spectrum. It is computed using the following expression (Drożdż and Oświęcimka 2015):

$$AI = \frac{\Delta\alpha_{left} - \Delta\alpha_{right}}{\Delta\alpha_{left} + \alpha_{right}} \tag{6}$$

where $\Delta\alpha_{left} = \alpha_0 - \alpha_{\min}$ and $\Delta\alpha_{right} = \alpha_{\max} - \alpha_{right}$ are respectively, the width of left and right limbs of the spectrum; their values depict the pattern of distributions of low and high fluctuations. The range of AI is $[-1, 1]$ and a positive AI value decipher a left-hand deviated spectrum, which might have resulted from local high fluctuations. A negative value of AI shows that the spectrum is right-hand deviated with local low fluctuations. If $AI = 0$, it characterizes a symmetrical multifractal spectrum. Singularity exponent for $q = 0$ (known as Hölder exponent α_0), indicates the complexity of the time series. High value of Hölder exponent indicates the time series is less correlated and possesses fine structure. On contrary, a low value of the Hölder exponent indicates that underlying process becomes correlated and loses its fineness, the appearance will be more regular (Krzyszczak et al. 2018).

3 Study Area and Database

The daily gridded data at a resolution of 0.25°x0.25° spatially is one of the finest scale rainfall information supplied by India Meteorological Department (IMD). The gridded rainfall data product was prepared by Pai et al. (2014) using varying network of 6955 rain gauge stations. There are specific tests reported in literature for quality control of daily meteorological datasets (Feng et al. 2004). But, as IMD performed statistical quality control measures before interpolation analysis, and compared the data with many global gridded data products and reported the superiority in the accurate representation of spatial rainfall variation, no additional tests are essential in this study. We have performed an overall quality check for its continuity and correctness and selected the data of the period of 1901–2013 for this study. This fine resolution data for long period of 1901–2013 (length of 41,272 days) is used in this study.

The spatial variability of multifractality is investigated by considering 34 meteorological subdivisions in India, defined by Indian Institute of Tropical Meteorology (IITM) Pune. Further, by aggregating the rainfall information and examining the rainfall homogeneity, IITM Pune defined six rainfall homogeneous regions in India. The non-overlapping rainfall homogeneous regions include Central Northeast India (CNEI), Hilly Regions (HR), Northeast India (NEI), Northwest India (NWI), Western Central India (WCI) and Peninsular India (PI). The map showing homogeneous rainfall regions in India is presented in Fig. 1.

It is well-evident that a Global climate shift occurred during 1976/77 period and some researchers have proved that the climate shift affected the pattern of Indian Summer Monsoon (Miller et al. 1994; Sahana et al. 2015). It is the strongest, most prominent and most debated and documented regime shifts and the persistence of the anomalous conditions was well-studied by the researchers in the last decade of the past century in particular (Trenberth 1990; Trenberth and Hurrell 1994). Different researchers reported a diverse set of parameters as the reason for such abrupt regime shift. The dynamics of the shift, both

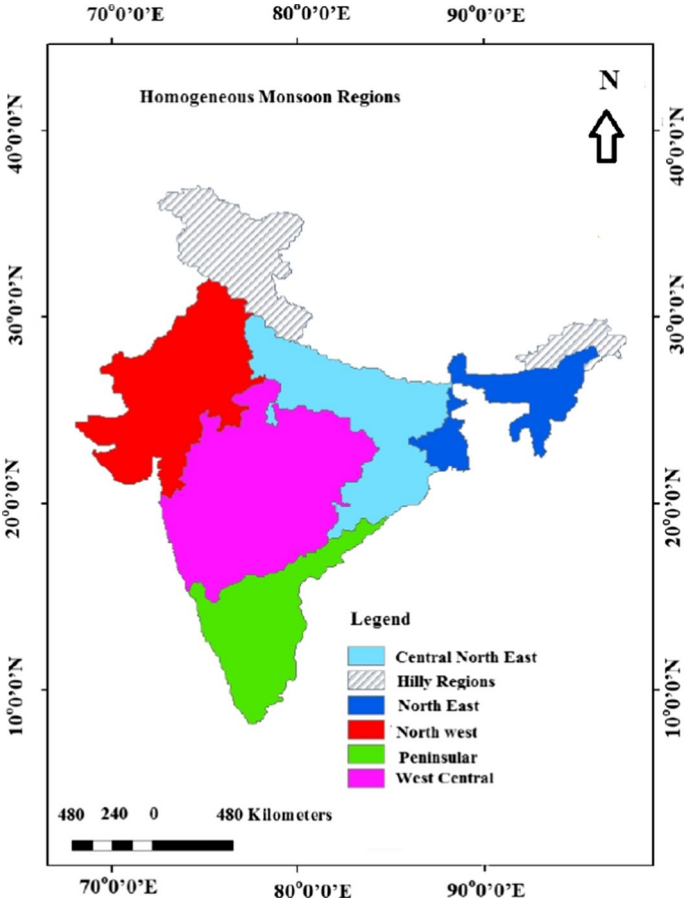

Fig. 1 Rainfall homogeneous regions of India

atmospheric and oceanic, were studied in detail by Miller et al. (1994). Graham (1994) identified that because of atmospheric teleconnections to the mid-latitudes, warming of sea surface temperature was resulted by remote forcing from the tropical Pacific Ocean. The differences in sea-level pressure (SLP), geo-potential height, temperature, wind, cloudiness, and precipitation are identified to be the variables for such multidecadal variations in Pacific region (Hartman and Wendler 2005). Wu et al. (2005) attributed the global climate shift to the coupled ocean–atmosphere interaction over the North Pacific in response to persistent wind stress anomalies in the previous decade. The coupled ocean–atmosphere mode in the North, mid-latitude stochastic forcing and extratropical– tropical interaction was recognized and reported as the drivers for such a regime shift (Wu et al., 2005). Powell and Xu (2012) investigated the role of global forcing mechanisms, including coupled solar and atmospheric dynamic forcing on Pacific climate shift of 1976/77. As the regime shift of 1976/77 is well evident, we have adopted this year as the recognized common change point year for all the grid points (>4800 points) to investigate the temporal variability of multifractal properties. The basic statistics of the dataset of the whole period (1901–2013),

Table 1 Descriptive statistics of rainfall over different rainfall homogeneous regions. MAR—Mean Annual rainfall; NNRD—Number of Non Rainy Days; PNRD—Percentage of Non-Rainy Days

Homogeneous region	1901–2013			Pre-1976/77			Post-1976/77		
	MAR	NNRD	PNRD	MAR	NNRD	PNRD	MAR	NNRD	PNRD
Central Northeast (CNE)	1199	28,993	70.25	1208	19,421	68.95	1177	9585	73.13
Hilly Region (HR)	1256	26,318	63.77	1212	18,241	64.76	1358	8005	61.08
Northeast (NE)	2185	21,214	51.40	2158	14,325	50.85	2248	6883	52.58
Northwest (NW)	538	35,114	85.08	538	23,572	83.68	539	11,550	88.13
West Central (WC)	1120	29,600	71.72	1133	19,730	70.05	1092	9896	75.51
Peninsular India (PI)	1240	28,455	68.94	1240	19,085	67.76	1241	9380	71.57

pre-climate shift (1901–1976) and post-climate shift (1977–2013) periods are provided in Table 1.

Table 1 shows that the data of all the three time slots comprises of long and continuous zero values varying from 51–88% (approximately) in different monsoon homogeneous regions. On considering the pre- and post-climate shift periods, it is noted that the mean annual rainfall of Hilly and Northeast regions increases. It is further noticed that the percentage of non-rainy days increases in all the regions except the Hilly region in the post-climate shift period, indicating drier conditions after the climatic shift.

4 Results and discussion

4.1 Spatial variability of Multifractal properties over India

In this study, first the MFDFA is employed for the characteristic analysis of daily gridded rainfall data of from 1901 to 2013. The analysis is performed by considering a moment order of − 4 to 4 to avoid any possible bias considering the long data, even though higher-order moments can be included in the analysis (Drożdż et al. 2019). The characteristics of the data show that the data comprises of long and continuous zero values (Table 1). This may lead to wrong conclusions on the persistence of the series. To avoid any such possible bias and wrong interpretations, the minimum scale is kept more than the longest stretch of continuous zero values (Drożdż et al. 2019). Similarly, the maximum scale is kept as $L/10$, where L is the data length, following the recommendations available in the literature (Ihlen 2012; Krzyszczak et al. 2017; Adarsh et al. 2020). The different multifractal parameters like Hurst exponent (H), the spread of GHE plot ($\Delta h(q)$), spectral width (W), Hölder exponent (α0), asymmetry index (AI), spread of singularity spectrum plot ($\Delta f(\alpha)$) are determined for all the identified 4896 grid points. The spatial distributions of different multifractal properties of rainfall data are shown in Fig. 2. The probability density functions (PDFs) of different properties are determined using the nonparametric kernel density estimator (Ghosh and Mujumdar 2007) and the plots are shown in Fig. 3.

From Fig. 2, rainfall of majority of the grid points displays short-term persistence. It is found that rainfall of 81.41% of the total grid points shows short-term persistence (STP) and that of only 6.96% grids shows strong long-term persistence ($H > 0.7$). The mean Hurst exponent is found to be 0.423 (with a standard deviation of 0.14), which is also in the range

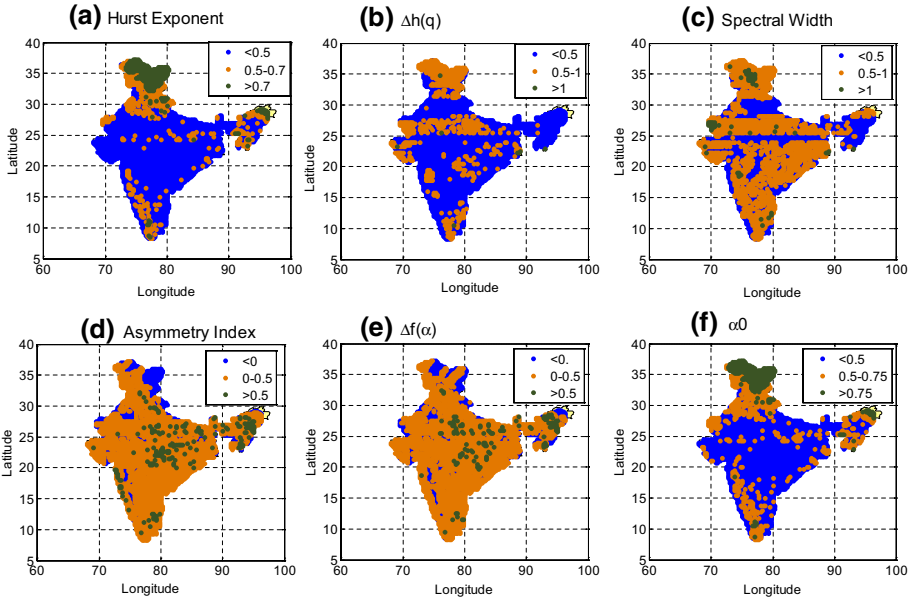

Fig. 2 Spatial distribution of different multifractal properties of rainfall data **a** Hurst exponent; **b** spread of GHE plot; **c** spectral width; **d** asymmetry index; **e** spread of singularity spectrum; **f** Hölder exponent

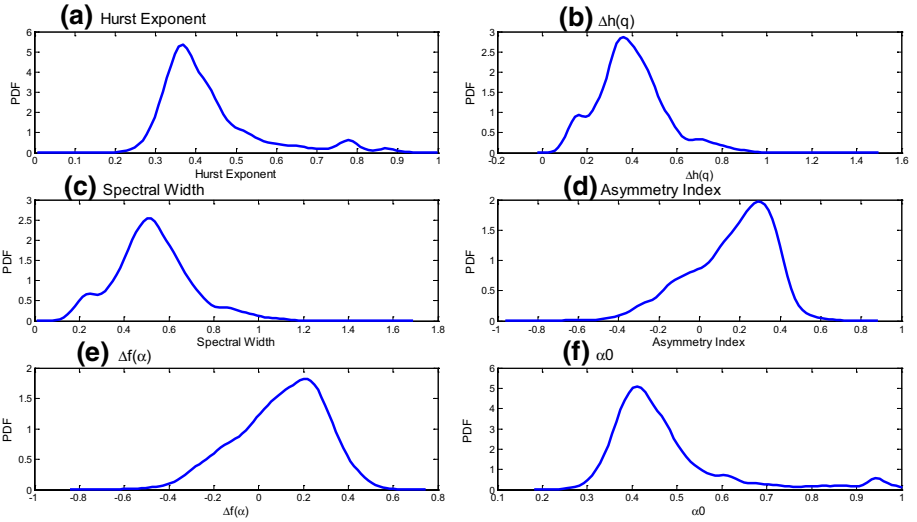

Fig. 3 PDFs of multifractal parameters of rainfall data **a** Hurst exponent; **b** spread of GHE plot; **c** spectral width; **d** asymmetry index; **e** spread of singularity spectrum; **f** Hölder exponent

of STP. From Fig. 2, it is noted that most of the grids showing LTP are concentrated in the Hilly regions of northern most and northeast regions of India. Even though the spread of GHE plot and spectral width (W) conveys similar information on the multifractality of the

series, the magnitudes of these parameters could differ, which resulted in different forms of spatial distribution. The mean values are found to be 0.358 and 0.493, respectively for $\Delta h(q)$ and spectral width (W). The distribution of Hölder exponent (Fig. 2f) is strikingly similar to that of Hurst exponent, this is due to the close association between the two parameters as reported by Burgueño et al. (2014) considering the daily temperature time series of Catelonia region, Spain. The correlation between the Hurst exponent and Hölder exponent in this database is found to be 0.98, which also supports the strong association between the two exponents. The mean Hölder exponent is 0.459 (with a variance of 0.025) which is quite close to that of Hurst exponent. The asymmetry of the multifractal spectrum of rainfall time series of each grid point is estimated by computing the asymmetry index (AI). It is found that about 78% of the grids (3820 grid points), the asymmetry index is positive, which indicates a right skewed spectrum showing relatively high fractal exponents with fine structure (Burgueño et al. 2014). This might have resulted from local high fluctuations, i.e., the singularity of the high values is larger than the low values. The spatial distribution of spread of singularity spectrum is also found to be displaying a fair degree of similarity with that of asymmetry index.

To gain insights of the multifractal properties of rainfall data in six rainfall homogeneous regions over India, the rainfall series of all grid points are segregated, and multifractal properties are estimated for them by the MFDFA method. PDFs and Cumulative distribution Functions (CDFs) of the multifractal properties are prepared and provided in Fig. 4.

From Fig. 4, it is clear that the values of Hurst exponent (H), spectral width (W) (and $\Delta h(q)$) and Hölder exponent are observed to be the highest in the hilly region and distinctly different from the values of the parameters of other regions. However, the asymmetry and ($\Delta f(\alpha)$) are found to be the lowest in the data of hilly region. In the NE region, the complexity is high (indicated by the values of Hölder exponent), but the degree of multifractality is the lowest. This may be because of the homogeneous distribution of rainfall in the

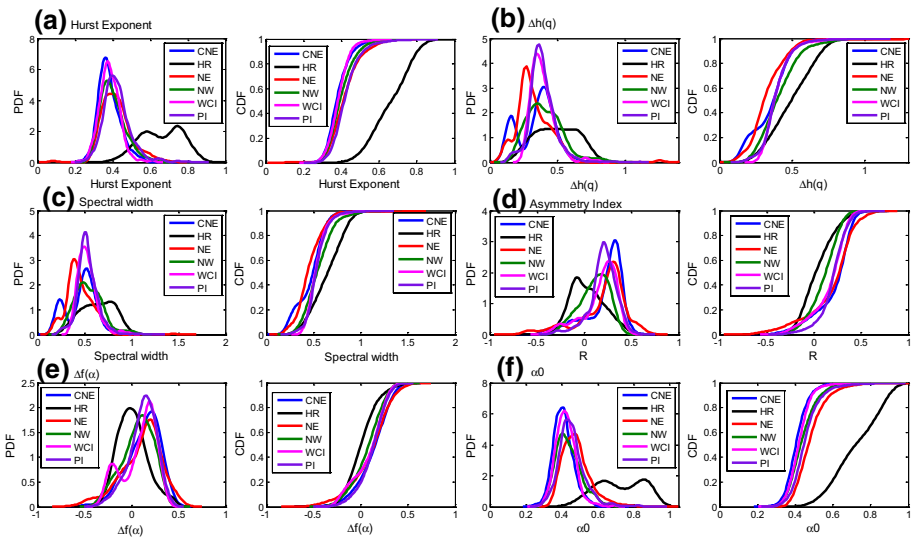

Fig. 4 PDFs and CDFs of different multifractal properties of rainfall data of different rainfall homogeneous regions **a** Hurst exponent; **b** spread of GHE plot; **c** spectral width; **d** asymmetry index; **e** spread of singularity spectrum; and **f** Hölder exponent

NE region. High density of degree of multifractality is noted (the values of spectral width (W) centered around 0.5) in the WCI and PI regions. The similarity in the PDFs and CDFs of Hölder exponent and Hurst exponent of different regions also confirm the strong association between the two exponents. To investigate the association between the Hölder exponent and Hurst exponent, the values of these parameters of different homogeneous regions are plotted and presented in Fig. 5.

Figure 5 shows that the strong association between Hurst exponent and Hölder exponent show good agreement in all the rainfall homogeneous regions in India (with an $R^2 > 0.9$) in all cases. This confirms that the association between the two exponents proved by Burgueño et al. (2014) based on daily temperature data is also applicable to the fine resolution daily rainfall time series if India could be adduced as a universality in the multifractal characterization of time series.

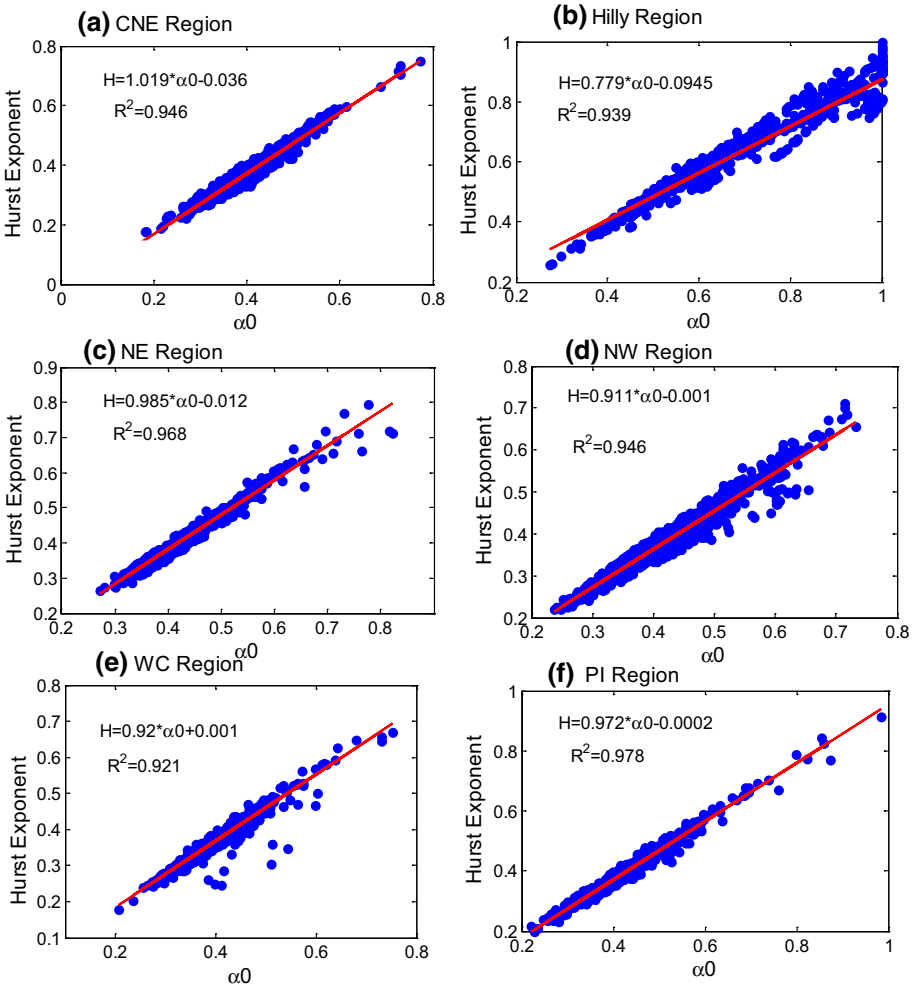

Fig. 5 Relation between Hurst exponent and Hölder exponent of rainfall time series of different homogeneous regions

For getting detailed information of the spatial distribution of multifractal properties of the rainfall over India, the variation of the properties over the six homogeneous regions and 34 meteorological subdivisions are analyzed. The statistical properties like mean, standard deviation (SD) and coefficient of variation (CV) of the three prominent multifractal parameters Hurst exponent, spectral width and Hölder exponent of rainfall data of six homogeneous regions are presented in Table 2 and similar results for the 34 subdivisions are provided in Table 3.

It is noticed that the persistence is highest in the Hilly region (with mean of 0.673) followed by NE region (with mean of 0.423, but the spatial variability of persistence is also the highest in these two regions (indicated by the CV value of ~ 23% for both regions). The rainfall pattern shows the highest multifractal degree in Hilly region and lowest in the NE region. Owing to the temporal homogeneity in rainfall, the multifractal degree of NE region might have dampened, but the pattern of rainfall among the different grid points shows distinct variability (indicated by the CV value). The variability of multifractal degree among the CNE region is also reasonably high (with a CV of 43%). On considering the complexity of the series (indicated by the Hölder exponent), the rainfall pattern of hilly region exhibits highest complexity and variability among the different grids (mean exponent of 0.74 and CV of 26%). Here, the standard deviation of values of Hölder exponent (0.198) of different grids is considerably larger than that of other regions. Rainfall of most of the grid points of Hilly region displays LTP (85% grids), whereas only 3% of rainfalls in the grids of WC region show LTP.

From Table 3, it is noted that the mean value of persistence is the highest at Jammu and Kashmir region, which belongs to the Hilly homogenous region. In the other subdivisions such as Arunachal Pradesh, Uttaranchal, Himachal Pradesh, which are part of Hilly homogenous region, also the mean persistence is relatively high (> 0.5). The smaller value of mean persistence is noted in regions like Gujarat, East Madhya Pradesh. Variability in the persistence is the highest at the Kerala meteorological subdivision (CV of 32%), whereas the variability of other subdivisions like Konkan and Goa, Coastal Karnataka also the variability is high. These two subdivisions belong to the Peninsular India, whereas rainfall of Arunachal Pradesh subdivision of Hilly homogeneous region is unique and shows high variability. The rainfall pattern of Vidarbha subdivision displayed lowest variability on persistence property (with standard deviation of 0.03 and CV of 11%). It is to be noted that this subdivision is one prominent drought-prone area in India (Ganguli and Janga Reddy 2013). The highest degree of multifractality is noticed in the records of Jammu and Kashmir and Western Rajasthan. These two are regions of distinctly different geographic and climatic patterns, where the former is moderate to high rainfall receiving region to the latter is an arid region. Again, in the Sikkim Sub-Himalaya, Uttaranchal and Haryana-Chandigadh-Delhi (HCD) regions, mean persistence is relatively low and mostly these regions belongs to Hilly homogeneous monsoon region. Therefore, it can be concluded that the multifractality is resulted because of the inherent pattern of the rainfall records, rather than the magnitude of the rainfall values. The highest variability in multifractality is noted in the Nagaland-Manipur-Mizoram–Tripura (NMMT) region and Western Uttar Pradesh region, in terms of the CV of W of different grid points. Degree of multifractality exhibits the least variability in regions of Peninsular India such as Rayalseema, Orissa, Coastal Anadhra Pradesh, Telengana and parts of the State of Karnataka. The behavior of mean degree of complexity and its variability is quite like that of Hurst Exponent, i.e., the mean value of H is also highest at Jammu and Kashmir, whereas the lowest at Gujarat and East Madhya Pradesh. Also, the highest variability is noticed at Kerala and lowest at the Vidarbha subdivisions. Table 3 further shows that rainfall of more than 50% of the grid points

Table 2 Statistical properties of multifractal parameters of rainfall data and statistics of LTP of rainfall in homogeneous regions of India. Largest values of each statistics are presented in bold and smallest values are given in italics

Number	Homogeneous region	Hurst Exponent			Spectral Width			Hölder Exponent			No of Grids with LTP in Rainfall	% of LTP in Rainfall
		Statistical Property			Statistical Property			Statistical Property				
		Mean	SD	CV (in %)	Mean	SD	CV (in %)	Mean	SD	CV (in %)		
1	Central Northeast (CNE)	*0.369*	0.073	19.652	0.451	0.194	43.049	*0.397*	0.069	17.410	45.000	5.275
2	Hilly Region (HR)	**0.673**	**0.157**	23.377	**0.629**	**0.247**	39.260	**0.743**	**0.198**	**26.593**	**595.000**	85.612
3	Northeast (NE)	0.423	0.099	**23.459**	*0.392*	0.189	**48.098**	0.447	0.098	21.913	69.000	16.953
4	Northwest (NW)	0.386	0.083	21.605	0.517	0.193	37.278	0.425	0.089	20.952	100.000	10.152
5	West Central (WC)	0.377	*0.067*	*17.735*	0.498	*0.130*	*26.032*	0.410	*0.068*	*16.638*	*24.000*	*3.768*
6	Peninsular India (PI)	0.403	0.089	22.057	0.502	0.134	26.596	0.433	0.091	20.895	70.000	11.058

Table 3 Statistical properties of multifractal parameters and statistics of LTP of rainfall data of meteorological subdivisions. Largest values of each statistics are given in bold and the smallest values are given in italics

No	Subdivision	Hurst exponent			Spectral width			Hölder exponent			No of Grids with LTP in Rainfall	% of grids with LTP in Rainfall
		Statistical property			Statistical property			Statistical property				
		Mean	SD	CV (in %)	Mean	SD	CV (in %)	Mean	SD	CV (in %)		
2	Arunachal Pradesh (AP)	0.563	**0.162**	28.677	0.423	0.099	23.312	0.587	**0.175**	29.843	65	55.552
3	Assam and Meghalaya (AM)	0.435	0.103	23.627	0.352	0.123	34.799	0.451	0.110	24.316	34	20.482
4	Nagaland Manipur Mizoram and Tripura (NMMT)	0.475	0.084	17.620	0.449	**0.348**	51.180	0.496	0.133	26.857	30	30.612
5	Sub Him West Bengal Sikkim (HBS)	0.377	0.069	18.332	0.340	0.150	44.101	0.395	0.067	16.839	2	3.333
6	Gangetic West Bengal (GWB)	0.373	0.087	23.333	0.583	0.230	39.460	0.425	0.062	14.650	3	3.448
7	Orissa (OR)	0.362	0.060	16.436	0.519	0.081	15.695	0.396	0.056	14.179	7	3.241
8	Jharkhand (JK)	0.360	0.075	20.978	0.430	0.199	46.262	0.389	0.073	18.676	5	4.386
9	Bihar (BH)	0.368	0.076	20.687	0.378	0.182	48.117	0.389	0.072	18.494	12	7.643
10	East Uttar Pradesh (EUP)	0.358	0.057	15.910	0.498	0.225	45.175	0.390	0.056	14.379	4	1.810
11	West Uttar Pradesh (WUP)	0.404	0.093	23.126	0.375	0.211	**56.304**	0.426	0.091	21.258	19	12.338
12	Uttaranchal (UA)	0.572	0.119	20.838	*0.284*	0.131	46.241	0.587	0.124	21.125	61	73.494
13	Haryana Chandigarh and Delhi (HCD)	0.461	0.097	21.109	0.311	0.094	30.306	0.480	0.099	20.553	21	30.000
14	Punjab (PB)	0.466	0.079	17.037	0.443	0.137	30.917	0.499	0.081	16.298	29	31.868
15	Himachal Pradesh (HP)	0.580	0.129	22.254	0.539	0.184	34.211	0.622	0.132	21.217	70	79.545
16	Jammu and Kashmir (JK)	**0.685**	0.121	17.713	**0.734**	0.197	26.880	**0.773**	0.167	21.631	**216**	**96.000**
17	West Rajasthan (WR)	0.397	0.063	15.858	0.681	0.193	28.285	0.457	0.077	16.746	21	9.333
18	East Rajasthan (ER)	0.351	0.057	16.214	0.462	0.186	40.318	0.382	0.059	15.471	4	1.932
19	West Madhya Pradesh (WMP)	0.357	0.053	14.758	0.392	0.137	35.047	0.379	0.053	13.918	2	0.889
20	East Madhya Pradesh (EMP)	0.347	0.061	17.518	0.365	0.161	44.033	0.367	0.059	16.201	5	2.551
21	Gujarat (GJ)	*0.339*	0.056	16.606	0.435	0.105	24.177	*0.365*	0.059	16.034	1	0.806
22	Saurashtra Kutch and Diu (SKD)	0.340	0.055	16.287	0.576	0.165	28.708	0.380	0.063	16.667	*0*	*00.000*
23	Konkan and Goa (KG)	0.379	0.096	25.218	0.419	0.094	22.443	0.401	0.098	24.485	7	10.000

Table 3 (continued)

No	Subdivision	Hurst exponent			Spectral width			Hölder exponent			No of Grids with LTP in Rainfall	% of grids with LTP in Rainfall
		Statistical property			Statistical property			Statistical property				
		Mean	SD	CV (in %)	Mean	SD	CV (in %)	Mean	SD	CV (in %)		
24	Madhya Maharastra (MM)	0.399	0.075	18.918	0.571	0.172	30.190	0.446	0.071	16.003	11	7.237
25	Marathwada (MW)	0.373	0.045	12.050	0.447	0.081	18.130	0.397	0.045	11.323	11	12.360
26	Vidarbha (VB)	0.344	*0.039*	*11.259*	0.460	0.111	24.156	0.372	*0.039*	*10.494*	11	8.029
27	Chhatisgarh (CG)	0.347	0.042	12.147	0.496	0.120	24.121	0.380	0.044	11.633	11	6.111
28	Coastal Andhra Pradesh (CoAP)	0.372	0.052	14.113	0.473	0.077	16.224	0.401	0.050	12.474	2	1.600
29	Telangana (TG)	0.356	0.054	15.181	0.485	0.081	16.773	0.387	0.053	13.814	2	1.333
30	Rayalaseema (RS)	0.387	0.053	13.666	0.506	*0.072*	*14.235*	0.421	0.051	12.155	3	3.333
31	Tamil Nadu and Pondicherry (TP)	0.419	0.098	23.280	0.584	0.163	27.981	0.453	0.103	22.674	21	12.000
32	Coastal Karnataka (CoK)	0.372	0.107	28.760	0.456	0.092	20.119	0.398	0.104	25.990	5	12.821
33	North Interior Karnataka (NIK)	0.421	0.048	11.515	0.520	0.088	16.975	0.455	0.050	11.098	7	6.731
34	South Interior Karnataka (SIK)	0.413	0.069	16.605	0.486	0.089	18.238	0.443	0.068	15.448	16	13.008
35	Kerala (KL)	0.444	0.145	**32.623**	0.389	0.171	43.782	0.462	0.149	**32.192**	22	33.846

of Himachal Pradesh, Uttaranchal, Jammu and Kashmir and Arunachal Pradesh shows LTP and all these subdivisions belongs to the Hilly homogeneous monsoon region. All the grid points of Saurashtra-Kutch-Diu (SKD) subdivision show STP and in the adjacent subdivisions like West Madhya Pradesh and Gujarat also, rainfall of most of the grid points displays STP.

4.2 Temporal variability of multifractal properties

To evaluate the temporal variability of multifractal properties, the complete data can be partitioned into sub-series and the MFDFA of each sub-series can be performed. However, it is anticipated that only a marginal change may get resulted in different multifractal properties over the time spells, if the time spells are of shorter duration, which may also lead to inconsistencies in results during the implementation of MFDFA. Also, there should be strong evidence of changes in rainfall patterns or non-stationarity in the time series of different spells. Keeping the above aspects in mind, it is decided to partition the rainfall time series of each grid point with respect to 1977. The signatures of a regime shift of climate in 1976/77 are well-debated in the literature (Graham 1994). Therefore, the rainfall time series of multifractal properties of pre- and post-1976/77 climate shift are examined for their multifractality. The CDFs of different multifractal parameters of rainfall time series for pre- and post-1977 Pacific climatic shift are presented in Fig. 6.

From Fig. 6, it is clear that there is an increase in multifractality of the series, while a mixed response is noted in the persistance and complexity of the series after the climate shift of 1977. This could also be linked with the changes indicated in the standardized precipitation index (SPI) series of post-1976/77 period (Adarsh et al. 2019). The asymmetry index (AI) and spread of multifractal spectrum ($\Delta f(\alpha)$) are fund to be reducted for the time

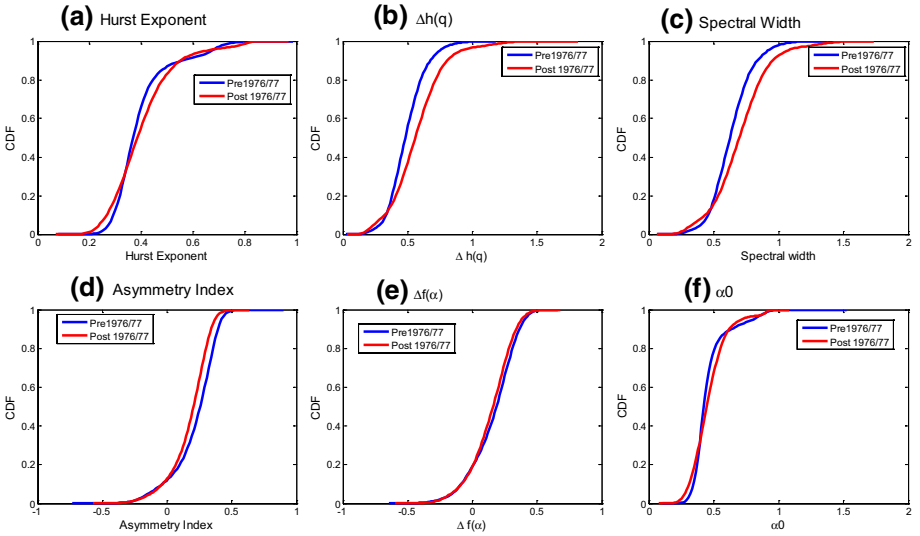

Fig. 6 CDFs of multifractal parameters of rainfall time series of pre- and post-1976/77 climate shift **a** Hurst exponent; **b** spread of GHE plot; **c** spectral width; **d** asymmetry index; **e** spread of singularity spectrum; and **f** Hölder exponent

series of post-1977 period when compared to the time series of pre-1977 period, even-though overall reduction is marginal. The three important properties which can contribute to the persistence, multifractality and complexity (H, W and α0) of time series are analyzed in detail and the spatial distributions of these parameters of pre- and post-1977 period are presented in Fig. 7. On considering the values of prominent multifractal properties (H W and α0) of the time series of post-1977 period with the pre-1977 period, an increase in multifractal properties was noted in 62% grid points while that for persistance and complexity showed a balance (50.2 and 54%, respectively).

The statistical properties of three prominent multifractal properties of the pre- and post-1977 rainfall time series are provided in Table 4.

Results presented in Table 4 show that overall, there is only marginal change in the mean, SD and CV values of different multifractal parameters of the pre- and post-1977 climate shift period. From Table 4, it is noted that the percentage changes in the mean of H, W and α0 are found to be 0.52, 8.03 and 1.6, whereas the percentage changes in the standard deviations are 16.5, 41.5 and 8.4, respectively. Number of grids with LTPs is found to be 797 in the post-1976/77 period, against 630 in the pre-1976/77 period. It is further noted that number of grid points showing LTP increased after the climate shift, even though this number is marginal. Again it is to be noted that the above statistics can give only an overall picture of the changes in the multifractal properties after the climatic shift. One cannot ignore the fact that such changes and transition from LTP to STP (or vice versa) can be local phenomenon. Such local (regional) changes will have significant impact in the basin or subdivisional scale hydrology.

Also, the changes are to be quantified in the context of urbanization and the climatic changes. Therefore, an attempt was made to find out the reduction in values of H, W and α0, which can give some inference on the effect of the plausible causes like urbanization on

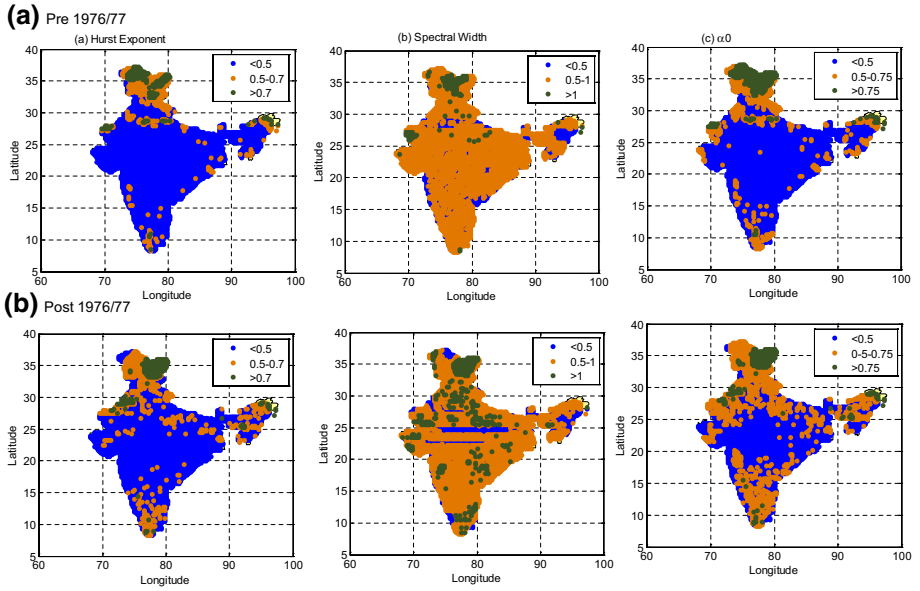

Fig. 7 Spatial distributions of multifractal parameters of the pre- and post-1977 rainfall time series data **a** Hurst exponent; **b** spectral width; and **c** Hölder exponent

Table 4 Statistical properties of the three prominent multifractal parameters of the pre- and post-1977 time series

Period	Hurst Exponent			Spectral Width			Hölder Exponent			No of Grids with LTP	% of LTP in Rainfall
	Statistical Property			Statistical Property			Statistical Property				
	Mean	SD	CV (In %)	Mean	SD	CV (In %)	Mean	SD	CV (In %)		
Pre-1976/1977	0.383	0.121	31.728	0.622	0.176	28.365	0.437	0.143	32.798	630	12.870
Post-1976/1977	0.385	0.141	36.644	0.672	0.249	37.023	0.444	0.155	34.876	797	16.282

the multifractal characteristics of the rainfall data, as the country experienced more urbanization in the recent past and it influenced the rainfall patterns and extremes (Shastri et al. 2015). The number of grids of homogeneous monsoon regions, with a reduction in the different multifractal parameters along with the percentage of grids which experienced a reduction are presented in Table 5.

From Table 5, it is noted that the highest percentage of grid points experienced a reduction in persistence and complexity is in the West Central India, whereas the reduction is multifractality is highest in the NE and NW regions. i.e., the rainfall characterizes became more homogeneous in these regions. This could be attributed to the urbanization in such a way that the urbanization has dominant effect in other four homogeneous regions than the NE and NW regions. It is noted that interestingly the reduction in persistence, complexity and multifractality is the least for the Peninsular region. The multifractal properties of rainfall could also be associated with the physical mechanisms resulting in the rainfall. The Peninsular region of India is bounded by the Bay of Bengal in the east, Indian Ocean in the south and Arabian Sea in the west. The proximity of ocean plays a dominant role in the rainfall of the country in general, and the Peninsular region. It was well-proven that the large scale oceanic climatic oscillations such as Quasi Biennial Oscillation (QBO), El-Niño Southern Oscillation (ENSO), Equatorial Indian Ocean Oscillation (EQUINOO), North Atlantic Oscillation (NAO), Atlantic Multi Decadal Oscillation (AMO) are playing a dominant role in Indian monsoon system (Gadgil et al. 2004; Goswami et al. 2006). Hence, the role of these circulations on the multifractality of the time series also cannot be ignored (Yu et al. 2014). Apart from the global parameters like terrestrial radiations and temperature the local factors like the latitude, topography, and local processes along with oceanic and atmospheric circulations may influence the multifractality of the rainfall series. However, it is very difficult to find the changes in the exponents with altitude, latitude, or coastal proximity (Yu et al. 2014). Also linking the cause of multifractality to single attribute is quite difficult, due to the high complexity of Indian monsoon system and the influence of many local or regional processes and particulars like terrain, moisture, vegetation, etc. on the local rainfalls. As the least reduction in the properties was noted in the Peninsular India, one can attribute it to the increased urbanization. The increased urbanization might have changed the rainfall pattern more heterogeneous and irregular in the regions other than NE and NW, the Peninsular India in particular. With the objective of a microscopic examination on the changes in different multifractal properties, the number of grids of the 34 meteorological subdivisions with a reduction in the different multifractal properties along with the percentage of grids which experienced a reduction are presented in Table 6.

From Table 6, it is noted that the highest reduction in the persistence and complexity are noted in subdivisions like Marathwada, Vidarbha, Chattisgarh, Konkan and Goa and parts of Madhya Pradesh. This was also reflected in computations made at the regional scale. The West Rajasthan (arid and desert dominated region) subdivision experienced least reduction in persistence properties, where the pattern of rainfall might not display any apparent change in the post-1977 period. The highest reduction in multifractality is noticed in the East Madhya Pradesh whereas the subdivisions like Telangana and Rayalaseema (which are the parts of Peninsular India) along with the Gangetic West Bengal displayed lesser percent reduction in multifractality. Apart from examining the reduction/increase in the multifractal properties, it is more rational to consider the switchover from STP to LTP (and vice versa) and positive to negative asymmetry (and vice versa). The former can give an insight on the predictability, while the latter one can give useful information on changing patterns like occurrences of hydrological extremes like flood or drought.

Table 5 Statistics of reduction in values of three prominent multifractal parameters of rainfall in homogeneous regions with respect to 1976/77 climatic shift

No	Homo-geneous region	Number of grids	Number of grids with reduction in H	Percentage of grids with reduction in H	Number of grids with reduction in W	Percentage of grids with reduction in W	Number of grids with reduction in value of α0	Percentage of grids with reduction in value of α0
1	CNE	853	368	43.142	333	39.039	336	39.390
2	HR	701	353	50.429	253	36.143	345	49.286
3	NE	403	184	45.658	189	**46.898**	166	41.191
4	NW	983	328	33.435	460	**46.891**	324	33.028
5	WC	1323	1000	**75.586**	496	37.491	897	**67.800**
6	PI	633	206	*32.543*	131	*20.695*	185	*29.226*

Table 6 Statistics of reduction in prominent multifractal properties (H, W and α0) with respect to 1976/77 climate shift in meteorological subdivisions

Number	Subdivision	Number of grids	Number of grids with reduction in H	Percentage of grids with reduction in H	Number of grids with reduction in W	Percentage of grids with reduction in W	Number of grids with reduction in α0	Percentage of grids with reduction in α0
2	AP	117	58	49.573	60	51.282	56	47.863
3	AM	166	58	34.940	108	65.060	57	34.337
4	NMMT	97	48	49.485	56	57.732	43	44.330
5	HBS	60	35	58.333	24	40.000	32	53.333
6	GWB	84	45	53.571	4	4.762	36	42.857
7	OR	216	98	45.370	35	16.204	80	37.037
8	JK	114	51	44.737	45	39.474	47	41.228
9	BH	157	57	36.306	105	66.879	61	38.854
10	EUP	221	73	33.032	113	51.131	68	30.769
11	WUP	154	92	59.740	37	24.026	81	52.597
12	UA	83	37	44.578	19	22.892	35	42.169
13	HCD	70	36	51.429	15	21.429	29	41.429
14	PB	91	36	39.560	41	45.055	33	36.264
15	HP	88	52	59.091	14	15.909	40	45.455
16	JK	411	207	50.365	160	38.929	214	52.068
17	WR	315	58	18.413	162	51.429	71	22.540
18	ER	207	95	45.894	110	53.140	91	43.961
19	WMP	247	205	82.996	149	60.324	205	82.996
20	EMP	196	146	74.490	138	70.408	155	79.082
21	GJ	124	51	41.129	58	46.774	56	45.161
22	SKD	178	54	30.337	77	43.258	47	26.404
23	KG	70	57	81.429	9	12.857	52	74.286
24	MM	152	105	69.079	45	29.605	82	53.947
25	MW	89	72	80.899	32	35.955	63	70.787
26	VB	137	123	89.781	52	37.956	113	82.482

Table 6 (continued)

Number	Subdivision	Number of grids	Number of grids with reduction in H	Percentage of grids with reduction in H	Number of grids with reduction in W	Percentage of grids with reduction in W	Number of grids with reduction in α0	Percentage of grids with reduction in α0
27	CG	180	142	78.889	47	26.111	120	66.667
28	CoAP	125	31	24.800	20	16.000	21	16.800
29	TG	150	89	59.333	2	1.333	62	41.333
30	RS	90	28	31.111	7	7.778	24	26.667
31	TP	175	62	35.429	41	23.429	60	34.286
32	CoK	39	14	35.897	8	20.513	15	38.462
33	NIK	104	64	61.538	18	17.308	47	45.192
34	SIK	123	38	30.894	22	17.886	36	29.268
35	KL	65	24	36.923	31	47.692	23	35.385

From the analysis on the switchover of persistence made by considering all the grid points, it is noticed that at 354 grid points the persistence changed from STP to LTP and at 187 grid points the change happened from LTP to STP, i.e., the status of persistence changed only in 544 (11% of the grid points) and in rest of the grid points the status remained the same. Further, the switchover from STP to LTP (and vice versa) was examined at regional and sub-divisional scale. Similarly, the switchover from positive to negative asymmetry (and vice versa) of multifractal spectra was also estimated. A switchover form negative to positive asymmetry is noted in 458 grid points and a switchover form positive to negative asymmetry is noted in 58 grid points, i.e., a total of 10% grids experienced a switchover in asymmetry. The results of switchover analysis of persistence and asymmetry are presented in Table 7.

From Table 7, it is noted that maximum percentage grids which subjected to a switch over in persistence is centered around 20. Interestingly, the maximum percentage if grid points which displayed a pattern change is in the Uttaranchal subdivision (24 and 23% grids respectively for a change from STP-LTP and vice versa respectively). Recollecting that a reasonably good percentage of grids in this region subjected to a reduction in properties like multifractality, persistence and complexity (23, 44 and 42%, respectively, in Table 6), it can be concluded that the pattern of rainfall in this region was vulnerable and might have subjected to a distinct change after 1977 climate shift. In the Kerala meteorological subdivision, the persistence property changed from short to long term in 23% grids, which also indicates a change in pattern of rainfall within the subdivision. On considering total number of grid points, the number of grids which displayed a right skewed spectrum was nearly same for the pre- and post-1977 periods (respectively 4292 and 4266). Percentage change in the number of grid points with left skewed to right skewed spectra was maximum for Hilly region subdivision and the change in switchover from right skewed to left skewed was maximum for NW region (33% and 15% in Table 7). This is reflected in the sub-divisional scale analysis also, as the maximum percentage of grids experienced a change from negative to positive asymmetry of the spectrum belongs to Jammu and Kashmir (JK), Himachal Pradesh (HP). Also, maximum percentage of grids experienced a switchover from positive to negative asymmetry was noted in subdivisions like West Madhya Pradesh (WMP), East Rajasthan (ER), SKD indicating more frequent occurrences of drought in these regions in the post-1977 period.

This study focused on the analysis of spatiotemporal variability of multifractal properties of rainfall considering a fine resolution data product. The global warming and climatic changes are influencing the hydrological water balance in different parts of the globe, which also believed to enhance the frequency of extreme events. The significant changes in the statistical estimates bring non-stationarity in the datasets, which could lead to erroneous predictions on following the conventional modeling practices. Any significant change in the persistence or multifractality may lead to inaccurate hydrological predictions and the situation is quite like the use of stationarity assumption under non-stationary condition. In this context, the spatiotemporal changes in the multifractal properties are to be monitored vigilantly particularly in a changing climate scenario.

Table 7 Statistics of switch over from STP to LTP (and vice versa) and positive asymmetry to negative asymmetry (and vice versa) of multifractal spectrum with respect to 1976/77 climate shift

ID	Subdivision	Number of Grids STP to LTP	Percentage of Grids (STP to LTP)	Number of Grids LTP to STP	Percentage of Grids (LTP to STP)	Number of Grids -AI to+AI	Percentage of Grids -AI to+AI	Number of Grids+AI to -AI	Percentageof Grids+AI to -AI
Subdivision									
2	AP	19	16.24	8	6.84	3	2.56	11	9.40
3	AM	30	18.07	3	1.81	12	7.23	15	9.04
4	NMMT	13	13.40	7	7.22	0	0.00	18	18.56
5	HBS	2	3.33	2	3.33	8	13.33	4	6.67
6	GWB	9	10.71	3	3.57	1	1.19	0	0.00
7	OR	1	0.46	9	4.17	2	0.93	1	0.46
8	JK	5	4.39	0	0.00	0	0.00	8	7.02
9	BH	10	6.37	2	1.27	0	0.00	18	11.46
10	EUP	27	12.22	5	2.26	16	7.24	13	5.88
11	WUP	2	1.30	15	9.74	40	25.97	9	5.84
12	UA	20	24.10	19	22.89	5	6.02	0	0.00
13	HCD	11	15.71	14	20.00	20	28.57	8	11.43
14	PB	17	18.68	0	0.00	4	4.40	10	10.99
15	HP	11	12.50	13	14.77	20	22.73	8	9.09
16	JK	25	6.08	59	14.36	203	49.39	51	12.41
17	WR	58	18.41	5	1.59	55	17.46	39	12.38
18	ER	7	3.38	0	0.00	5	2.42	43	20.77
19	WMP	0	0.00	0	0.00	6	2.43	52	21.05
20	EMP	1	0.51	0	0.00	1	0.51	31	15.82
21	GJ	3	2.42	0	0.00	4	3.23	7	5.65
22	SKD	7	3.93	0	0.00	2	1.12	45	25.28
23	KG	1	1.43	3	4.29	0	0.00	3	4.29
24	MM	0	0.00	4	2.63	2	1.12	45	25.28

Table 7 (continued)

ID	Subdivision	Number of Grids STP to LTP	Percentage of Grids (STP to LTP)	Number of Grids LTP to STP	Percentage of Grids (LTP to STP)	Number of Grids -AI to + AI	Percentage of Grids -AI to + AI	Number of Grids + AI to -AI	Percentageof Grids + AI to -AI
25	MW	1	1.12	0	0.00	15	16.85	4	4.49
26	VB	0	0.00	0	0.00	3	2.19	0	0.00
27	CG	0	0.00	0	0.00	0	0.00	4	2.22
28	CoAP	6	4.80	1	0.80	2	1.60	0	0.00
29	TG	1	0.67	0	0.00	1	0.67	1	0.67
30	RS	1	1.11	2	2.22	2	2.22	3	3.33
31	TP	32	18.29	7	4.00	5	2.86	9	5.14
32	CoK	1	2.56	1	2.56	0	0.00	2	5.13
33	NIK	5	4.81	0	0.00	6	5.77	19	18.27
34	SIK	13	10.57	1	0.81	14	11.38	13	10.57
35	KL	15	23.08	4	6.15	1	1.54	5	7.69
Homogeneous regions									
1	CNE	45	5.28	30	3.52	57	6.68	50	5.86
2	HR	74	10.57	99	14.14	231	33.00	69	9.86
3	NE	54	13.40	15	3.72	21	5.21	37	9.18
4	NW	104	10.60	20	2.04	91	9.28	151	15.39
5	WC	8	0.60	7	0.53	48	3.63	155	11.72
6	PI	69	10.90	16	2.53	24	3.79	35	5.53

5 Conclusion

In this study, the multifractality of fine resolution daily rainfall fields over India are evaluated using MFDFA method. A rigorous evaluation on the spatiotemporal variability of different multifractal properties is performed. The fine resolution (0.25°x0.25°) daily gridded rainfall data of India exhibited multifractal behavior with majority of the grid points (about 81%) possessing short-term persistency. The highest multifractal degree, persistence and complexity is noted in the hilly terrains of northern and northeastern India, where in most of the grids, the rainfall time series displayed long-term persistence. The multifractal spectra of the rainfall time series of most of the grid points (78%) are right skewed indicating fine structured and complex characteristics. An increase in multifractality noticed for the post-1976/77 time series in majority of the grid points (62%), while the changes in complexity and persistence was marginal. Changes in the status of persistence with respect to 1976/77 is the highest at Uttaranchal subdivision and changes from positive to negative asymmetry was the highest at NW region indicating increased frequency of drought occurrences. Grid points of Peninsular India exhibited least reduction in complexity, multifractality and persistence in the post-1977 period when compared to pre-1977 period.

Acknowledgement The authors acknowledge the service of India meteorological Department (IMD) for providing the 0.25°× 0.25° daily rainfall time series for performing this research work.

References

Adarsh S, Dharan DS, Anuja PK, Suman A (2018) Unravelling the scaling characteristics of daily streamflows of Brahmani river basin. SN Applied Sciences, India using Arbitrary Order Hilbert Spectral and Detrended Fluctuation Analyses. https://doi.org/10.1007/s42452-018-0056-1

Adarsh S, Nagesh Kumar D, Deepthi B, Gayathri G, Aswathy SS, Bhagyasree S (2019) Multifractal characterization of meteorological drought in India using detrended fluctuation analysis. Int J Climatol 39(11):4234–4255

Adarsh S, Nourani V, Archana DS, Dharan DS (2020) Multifractal description of rainfall fields over India. J Hydrol. 586:124913. https://doi.org/10.1016/j.jhydrol.2020.124913

Ali M, Deo RC, Downs NJ, Maraseni T (2018a) An ensemble-ANFIS based uncertainty assessment model for forecasting multi-scalar standardized precipitation index. Atmos Res 207:155–180

Ali M, Deo RC, Maraseni T, Downs NJ (2019) Improving SPI-derived drought forecasts incorporating synoptic-scale climate indices in multi-phase multivariate empirical mode decomposition model hybridized with simulated. J Hydrol 576:164–184

Ali M, Deo RC, Downs NJ, Maraseni T (2018b) Multi-stage committee based extreme learning machine model incorporating the influence of climate parameters and seasonality on drought forecasting. Comput Electron Agric 152:149–165

Baranowski P, Krzyszczak J, Slawinski C, Hoffmann H, Kozyra J, Nieróbca A, Siwek K, Gluza A (2015) Multifractal analysis of meteorological time series to assess climate impacts. Clim Res 65:39–52

Barredo JI (2007) Major flood disasters in Europe: 1950–2005. Nat Hazards 42(1):125–148

Bhalme HN, Mooley DA (1980) Large-scale droughts/floods and monsoon circulation. Mon Weather Rev 108(8):1197–1211

Burgueño A, Lana X, Serra C, Martínez MD (2014) Daily extreme temperature multifractals in Catalonia (NESpain). Phys Lett A 378(2014):874–885

Chattopadhyay J, Bhatla R (2002) Possible influence of QBO on teleconnections relating Indian summer monsoon rainfall and sea-surface temperature anomalies across the equatorial pacific. Int J Climatol 22(1):121–127

Dahlstedt K, Jensen H (2005) Fluctuation spectrum and size scaling of river flow and level. Phys A 348:596–610

Deidda R, Benzi R, Siccardi F (1999) Multifractal modeling of anomalous scaling laws in rainfall. Wat Resour Res 35(6):1853–1867

Deidda R (1999) Multifractal analysis and simulation of rainfall fields in space. Phys Chem Earth: Part B. Hydrol Oceans Atmos 24:73–78
Deidda R (2000) Rainfall downscaling in a space-time multifractal framework. Wat Resour Res 36(7):1779–1794
Drożdż S, Oświęcimka P, (2015) Detecting and interpreting distortions in hierarchical organization of complex time-series. Phys Rev E 91:030902
Drożdż S, Minati L, Oświęcimka P, Stanuszek M, Wątorek M (2019) Signatures of the crypto-currency market decoupling from the Forex. Future Internet 11(7):154. https://doi.org/10.3390/fi11070154
Feng S, Hu Q, Qian Q (2004) Quality control of daily meteorological data in China, 1951–2000: A new dataset. Int J Climatol 24:853–870
Gadgil S, Vinayachandran PN, Francis PA, Gadgil S (2004) Extremes of the Indian summer monsoon rainfall, ENSO and equatorial Indian Ocean oscillation. Geophys Res Lett 31:L12213. https://doi.org/10.1029/2004GL019733
Ganguli P, Janga Reddy M (2013) Evaluation of trends and multivariate frequency analysis of droughts in three meteorological subdivisions of Western India. Int J Climatol 34(3):911–928
Garcia-Marin AP, Estevez J, Medina-Cobo MT, Ayuso-Munoz JL (2015) Delimiting homogeneous regions using the multifractal properties of validated rainfall data series. J Hydrol 529:106–119
Garcia-Marin AP, Morbidelli R, Saltalippi C, Cifrodelli M, Estevez J, Flammini A (2019) On the choice of the optimal frequency analysis of annual extreme rainfall by multifractal approach. J Hydrol 575(2019):1267–1279
Ghosh S, Mujumdar PP (2007) Non-parametric methods for modeling GCM and scenario uncertainty in drought assessment. Wat Resour Res. https://doi.org/10.1029/2006WR005351
Goswami BN, Madhusoodanan MS, Neema CP, Sengupta D (2006) A physical mechanism for North Atlantic SST influence on the Indian summer monsoon. Geophys Res Lett 33:L02706. https://doi.org/10.1029/2005GL024803
Graham NE (1994) Decadal scale variability in the 1970's and 1980's: Observations and model results. Clim Dyn 10:60–70
Hartmann B, Wendler G (2005) The Significance of the 1976 Pacific Climate Shift in the Climatology of Alaska. J Clim 18(22):4824–4839
Hou W, Feng G, Yan P, Li S (2018) Multifractal analysis of the drought area in seven large regions of China from 1961 to 2012. Meteorol Atmos Phys 130:459–471
Huang Y, Schmitt FG, Lu Z, Liu Y (2009) Analysis of daily river flow fluctuations using empirical mode decomposition and arbitrary order Hilbert spectral analysis. J Hydrol 373:103–111
Huang Q, Chen Y, Xu S, Liu J (2014) Case study of applying Multifractal models for rainfall IDF analysis in China. J Hydrol Engng 19(1):205–210
Hubert P (2001) Multifractals as a tool to overcome scale problems in hydrology. Hydrol Sci J 46(6):897–905
Hurst HE (1965) Long-term storage: An experimental study. Constable, London
Hurst HE (1951) Long-term storage capacity of reservoirs. Transaction of American Society of Civil Engineers 116:770–808
Ihlen EAFE (2012) Introduction to multifractal detrended fluctuation analysis in MATLAB. Front physiol 3:141
Kantelhardt JW, Koscielny-Bunde E, Rybski D, Braun P, Bunde A, Havlin S (2006) Long-term persistence and multifractality of rainfall and river runoff records. J Geophys Res. https://doi.org/10.1029/2005JD005881
Kantelhardt JW, Zschiegner SA, Koscielny-Bunde E, Havlin S, Bunde A, Stanley HE (2002) Multifractal detrended fluctuation analysis of non-stationary time series. Phys A 316(1–4):87–114
Kantelhardt JW, Rybski D, Zschiegner SA, Braun P, Koscielny-Bunde E, Livina V, Havlin S, Bunde A (2003) Multifractality of river runoff and rainfall: comparison of fluctuation analysis and wavelet methods. Phys A 330:240–245
Karatasou S, Santamouris M (2018) Multifractal analysis of high-frequency temperature time series in the urban environment. Climate 6(2):50
Kolmogorov AN (1941) Local structure of turbulence in an incompressible liquid for very large Reynolds numbers. Proc Acad Sci URSS Geochem Sect 30:299–303
Koscielny-Bunde E, Kantelhart JW, Braun P, Bunde A, Havlin S (2006) Long-term persistence and multifractality of river runoff records: detrended fluctuation studies. J Hydrol 322:120–137
Krzyszczak J, Baranowski P, Zubik M, Hoffmann H (2017) Temporal scale influence on multifractal properties ofagro-meteorological time series. Agri Forest Meteorol 239(2017):223–235

Krzyszczak J, Baranowski P, Zubik M, Kazandjiev V, Georgieva V, Sławiński C, Siwek K, Kozyra J, Nieróbca A (2018) Multifractal characterization and comparison of meteorological time series from two climatic zones. Theo Appl Climatol. https://doi.org/10.1007/s00704-018-2705-0

Langridge R, Christian-Smith J, Lohse K (2006) Access and resilience: analyzing the construction of social resilience to the threat of water scarcity. Ecology and Society. https://doi.org/10.5751/ES-01825-110218

Li E, Mu X, Zhao G, Gao P (2015) Multifractal detrended fluctuation analysis of streamflow in Yellow river basin, China. Water 7:1670–1686

Mandelbrot B (1982) The fractal geometry of nature. WH Freeman Publishers, New York

Miller AJ, Rayan DR, Barnett TP, Graham NE, Oberhuber JM (1994) The 1976–77 Climate Shift of the Pacific Ocean. Oceanography 7(1):21–26

Obukhov AM (1949) Structure of the temperature field in a turbulent flow. Izv. Akad. Nauk. S.S.S.R Ser. Geogr Geofiz 13:58–69

Olsson J, Niemczynowicz J (1996) Multifractal analysis of daily spatial rainfall distributions. J Hydrol 187(1–2):29–43

Pandey G, Lovejoy S, Schertzer D (1998) Multifractal analysis of daily river flows including extremes for basins five to two million square kilometers, one day to 75 years. J Hydrol 208:62–81

Pathirana P, Herath S, Yamada T (2007) Estimating rainfall distributions at high temporal resolutions using a multifractal model. Hydrol Earth Sys Sci Disc 7(5):668–679

Pai D, Sridhar L, Rajeevan M, Sreejith O, Satbhai N, Mukhopadhyay B (2014) Development of a new high spatial resolution (0.25 × 0.25) long period (1901–2010) daily gridded rainfall data set over India and its comparison with existing data sets over the region. Mausam 65:1–18

Peng CK, Buldyrev SV, Havlin S, Simons M, Stanley HE, Goldberger AL (1994) Mosaic organization of DNA nucleotides. Physical rev E 49(2):1685

Powell AM Jr, Xu J (2012) The 1977 Global Regime Shift: A Discussion of Its Dynamics and Impacts in the Eastern Pacific Ecosystem. Atmos Ocean 50(4):421–436

Rego CRC, Frota HO, Gusmao MS (2013) Multifractality of Brazilian rivers. J Hydrol 495:208–215

Schertzer D, Lovejoy S (1987) Physical modelling and analysis of rain and clouds by aniso–tropic scaling multiplicative processes. J Geophys Res 92:9693–9714

Sahana AS, Ghosh S, Ganguly A (2015) Murtugudde R (2015) Shift in Indian summer monsoon onset during 1976/1977. Environ Res Lett 10:054006

Shang P, Kame S (2005) Fractal nature of time series in the sediment transport phenomenon. Chaos Solitons Fractals 26:997–1007

Shastri H, Paul S, Ghosh S, Karmakar S (2015) Impacts of urbanization on Indian summer monsoon rainfall extremes. J Geophys Res Atmos 120:495–516

Serinaldi F (2010) Multifractality, imperfect scaling and hydrological properties of rainfall time series simulated by continuous universal multifractal and discrete random cascade models. Nonlin Processes Geophys 17(6):697–714

Tan X, Gan TW (2017) Multifractality of Canadian rainfall and streamflow. Int J Climatol 37(S1):1221–1236

Tessier Y, Lovejoy S, Schertzer D (1993) Universal multifractals: Theory and observations for rain and clouds. J Appl Meteorol 32(2):223–250

Tessier Y, Lovejoy S, Hubert P, Schertzer D, Pecknold S (1996) Multifractal analysis and modeling of rainfall and river flows and scaling, causal transfer functions. J Geophys Res 101:26427–26440

Trenberth KE (1990) Recent observed interdecadal climate changes in the northern hemisphere. Bull Am Meteorol Soc 71:988–993

Trenberth KE, Hurrell JW (1994) Decadal atmosphere-ocean variations in the Pacific. Clim Dyn 9:303–319

Veneziano A, Furcolo P (2002) Multifractality of rainfall and scaling of intensity-duration-frequency curves. Wat Resour Res 38(12):1–12

Verrier S, de Montera L, Barthès L, Mallet C (2010) Multifractal analysis of African monsoon rain fields, taking into account the zero rain-rate problem. J Hydrol 389:111–120

Vörösmarty CJ et al (2010) Global threats to human water security and river biodiversity. Nature 467(7315):555–561

Yu ZG, Leung Y, Chen YD, Zhang Q, Anh V, Zhou Y (2014) Multifractal analyses of daily rainfall time series in Pearl River basin of China. Phys A 405:193–202

Wu L, Lee DE, Liu Z (2005) The 1976/77 North Pacific climate regime shift the role of subtropical ocean adjustment and coupled ocean-atmosphere feedbacks. J Climate. 18(23):5125–5140

Zhang Q, Xu C-Y, Chen YD, Yu Z (2008) Multifractal detrended fluctuation analysis of streamflow series of the Yangtze river basin, China. Hydrol Process 22:4997–5003

Zhang Q, Xu C-Y, Yu Z, Liu C-L, Chen Y-D (2009) Multifractal analysis of streamflow records of the East river basin (Pearl river), China. Phys A 388:927–934

Authors and Affiliations

Adarsh Sankaran[1] · Sagar Rohidas Chavan[2] · Mumtaz Ali[3] · Archana Devarajan Sindhu[1] · Drisya Sasi Dharan[1] · Muhammad Ismail Khan[4]

Adarsh Sankaran
adarsh_lce@yahoo.co.in

Sagar Rohidas Chavan
sagar@iitrpr.ac.in

Archana Devarajan Sindhu
archanadevarajan00@gmail.com

Drisya Sasi Dharan
drisyasdharan@gmail.com

Muhammad Ismail Khan
m.khan8@uq.edu.au

1 TKM College of Engineering Kollam, Kerala 691005, India

2 Indian Institute of Technology, Ropar, India

3 Deakin-SWU Joint Research Centre On Big Data, School of Information Technology, Deakin University, Victoria 3125, Australia

4 University of Queensland, Brisbane, Australia